Adiabatic formation of quasibound states of antihydrogen

C. E. Correa, J. R. Correa, and C. A. Ordonez
Department of Physics, University of North Texas, Denton, Texas 76203, USA
(Received 8 April 2005; revised manuscript received 18 July 2005; published 28 October 2005)

The classical trajectory of an initially unbound positron within the electric field of an antiproton and a uniform magnetic field is simulated in three dimensions. Several simulations are run incorporating experimental parameters used for antihydrogen production, which has been achieved by two different groups [M. Amoretti *et al.*, Nature (London) **419**, 456 (2002); G. Gabrielse *et al.*, Phys. Rev. Lett. **89**, 213401 (2002)]. The simulations indicate that temporary bound states of antihydrogen can form at positive energies, where the energy of the system is defined to be zero when the positron and antiproton are at rest with infinite separation. Such quasibound states, which form only when the magnetic field is present, are typically smaller than 0.4 μm in a dimension perpendicular to the magnetic field. An analytical model is developed for a formation cross section, and it is found that quasibound states may form more frequently than stable Rydberg states.

DOI: 10.1103/PhysRevE.72.046406 PACS number(s): 52.27.Jt, 52.20.Dq, 52.20.Fs, 52.65.Cc

I. INTRODUCTION

Antihydrogen atoms have recently been produced using nested Penning traps by the experimental groups ATRAP and ATHENA [1–4]. Under certain conditions, nested Penning traps allow for two oppositely signed plasma species to be confined with overlapping confinement regions using a uniform magnetic field and a superimposed electric field [5–7]. In the antihydrogen production experiments, antiprotons are made to interact with a positron plasma, and antihydrogen atoms have been reported to be produced in weakly bound states [8]. Various processes involving weakly bound hydrogen and antihydrogen atoms in a magnetic field are considered theoretically in Refs. [9–18]. Of particular note is the work reported in Refs. [16,17], where classical trajectory simulations, which employed the guiding center approximation, were used to simulate three-body recombination with initially unbound particles. In other work, classical trajectory simulations of two-body interactions between charged particles in a magnetic field were reported, and the chaotic nature of the interactions was investigated [19,20]. In the work presented here, a binary interaction between a positron and an antiproton within a uniform magnetic field is investigated using parameters that are typical of the antihydrogen production experiments. A preliminary summary of the work presented here was reported elsewhere [21]. Section II describes the development of a computer simulation of the classical trajectory of an initially unbound positron that encounters an antiproton in the presence of a uniform magnetic field. The full three-dimensional motion of the positron is simulated. (Thus, the guiding center approximation is not used.) It is found that a binary interaction between an initially unbound positron and an antiproton can result in the formation of a quasibound state of antihydrogen. No energy is transferred to or from the two-body system in the simulation. The physical basis for the formation of quasibound antihydrogen states is discussed. In Sec. III, an analytical expression that can be used to calculate an approximate cross section for the formation of quasibound states is obtained. The expression is compared to simulation results, and reasonable agreement with simulation results is found. A discussion of time scales is also presented. First, it is shown that the formation of quasibound states can increase the positron and antiproton interaction time substantially compared to the interaction time in the absence of an external magnetic field. Next, an expression for an approximate time scale associated with the rate of formation of quasibound antihydrogen states is obtained and is compared to a three-body recombination time scale. A brief discussion of two possible effects that quasibound state formation may have on antihydrogen production experiments is provided in Sec. IV, along with a concluding summary.

II. CLASSICAL TRAJECTORY SIMULATION

To compute the trajectory of a positron near an antiproton, the motion of the positron is treated classically, and the antiproton is approximated as a fixed point particle. A coordinate system is defined with the origin at the antiproton, and the position of the positron is denoted with the vector $\boldsymbol{r}=x\hat{\boldsymbol{i}}+y\hat{\boldsymbol{j}}+z\hat{\boldsymbol{k}}$. The force on the positron due to the electric field of the antiproton is $\boldsymbol{F}_E=(k_C q_1 q_2 \boldsymbol{r}/r^3)$, where $k_C=1/(4\pi\epsilon_0)$ is the Coulomb force constant (SI units are used), and q_1 and q_2 are the charges of the positron and the antiproton, respectively. A magnetic field, $\boldsymbol{B}=B\hat{\boldsymbol{k}}$, acts on the positron with a force given by $\boldsymbol{F}_B=k_L q_1(\boldsymbol{v}\times\boldsymbol{B})$, where k_L is the Lorentz force constant ($k_L=1$ in SI units) and $\boldsymbol{v}=\boldsymbol{r}'$ is the positron velocity. The total force acting on the positron is related to its acceleration by $\boldsymbol{F}_E+\boldsymbol{F}_B=m_1\boldsymbol{a}$, where m_1 is the positron mass and $\boldsymbol{a}=\boldsymbol{r}''$ is the positron acceleration. The equations of motion are

$$x''=\frac{k_C q_1 q_2 x}{m_1(x^2+y^2+z^2)^{3/2}}+\frac{k_L q_1 B v_y}{m_1}, \tag{1}$$

$$y''=\frac{k_C q_1 q_2 y}{m_1(x^2+y^2+z^2)^{3/2}}-\frac{k_L q_1 B v_x}{m_1}, \tag{2}$$

and

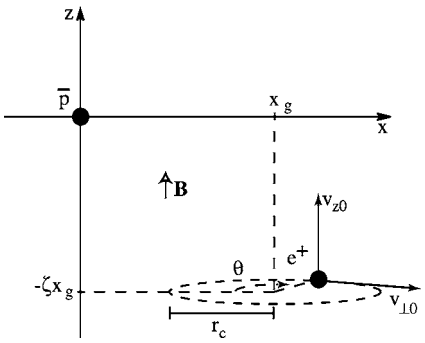

FIG. 1. Positron position at $t=0$. The y axis points into the page.

$$z'' = \frac{k_C q_1 q_2 z}{m_1 (x^2 + y^2 + z^2)^{3/2}}. \tag{3}$$

The simulation of the positron motion begins at time $t=0$, and the positron begins by following a helical path as a result of the presence of the magnetic field. The position coordinates and velocity components at $t=0$ are written as (see Fig. 1):

$$x(0) = x_0 = x_g - r_c \cos(\theta), \tag{4}$$

$$y(0) = y_0 = r_c \sin(\theta), \tag{5}$$

$$z(0) = z_0 = -\zeta x_g, \tag{6}$$

$$x'(0) = v_{x0} = v_{\perp 0} \sin(\theta), \tag{7}$$

$$y'(0) = v_{y0} = v_{\perp 0} \cos(\theta), \tag{8}$$

and $z'(0)=v_{z0}$. (An expression for v_{z0} is derived in the next paragraph.) Here, the following parameters are defined at $t=0$: x_g is the guiding center impact parameter, θ is an angle on the $z=z_0$ plane that specifies the positron's azimuthal location about the positron's guiding center (located at $x=x_g$, $y=0$), ζ is the normalized magnitude of z_0 and its value is chosen to be much greater than unity ($\zeta \gg 1$), $r_c=m_1 v_{\perp 0}/(k_L q_1 B)$ is the cyclotron radius, and $v_{\perp 0}=\sqrt{v_{x0}^2+v_{y0}^2}$ is the azimuthal velocity. It is also useful to refer to times $t \neq 0$, when the positron cyclotron radius is given by $m_1 v_\perp/(k_L q_1 B)$, where $v_\perp=\sqrt{v_x^2+v_y^2}$. However, the positron cyclotron radius and the positron guiding center (i.e., the positron position averaged over the cyclotron motion) are referred to only when the positron is sufficiently far from the antiproton for the positron to undergo near circular motion in the two dimensions perpendicular to the magnetic field. The restriction $r_c < x_g$ is employed to only consider cases where the antiproton is located outside of the positron cyclotron orbit projected onto the $z=0$ plane at $t \approx 0$. Thus, with Eqs. (4) and (6), the conditions $\zeta \gg 1$ and $r_c < x_g$ require that $|z_0| \gg x_0 > 0$. The positron energy at $t=0$ is

$$E_0 = \tfrac{1}{2} m_1 v_0^2 + \frac{k_C q_1 q_2}{r_0}, \tag{9}$$

where $v_0=\sqrt{v_{x0}^2+v_{y0}^2+v_{z0}^2}$ and $r_0=\sqrt{x_0^2+y_0^2+z_0^2}$.

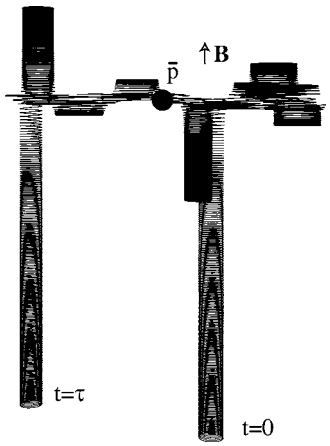

FIG. 2. Three-dimensional parametric plot of a positron trajectory in the electric field of an antiproton and in a uniform magnetic field. The $\hat{\boldsymbol{k}}$ dimension, which is parallel to $\boldsymbol{B}$, is reduced by a factor of 46 relative to the $\hat{\boldsymbol{i}}$ and $\hat{\boldsymbol{j}}$ dimensions.

Define r_i as a distance of separation between the positron and antiproton that is large enough for their interaction to be neglected. The limit that r_i approaches infinity is taken, the positron potential energy is defined to be zero at $r=r_i$, and the associated total energy is $E_i=K_i=\frac{1}{2}m_1(v_{xi}^2+v_{yi}^2+v_{zi}^2)$. The components of the positron velocity at $r=r_i$ are written as $v_{xi}=\eta_x v_{th}$, $v_{yi}=\eta_y v_{th}$, and $v_{zi}=\eta_z v_{th}$, where η_x, η_y, and η_z are normalized velocity components, $v_{th}=\sqrt{k_B T/m_1}$ is the positron thermal speed, T is the positron plasma temperature, and k_B is Boltzmann's constant. The value of the parameter ζ is chosen large enough that the positron perpendicular kinetic energy, which is defined as kinetic energy associated with motion perpendicular to the magnetic field, $K_\perp=\frac{1}{2}m_1 v_\perp^2$, remains approximately constant for a positron traveling from distances of separation r_i to distances of separation r_0. (Such motion is not simulated.) The approximation $K_{\perp i}=K_{\perp 0}$ (that is, $v_{\perp i}^2=v_{xi}^2+v_{yi}^2=v_{x0}^2+v_{y0}^2=v_{\perp 0}^2$) leads to

$$v_{\perp 0} = \sqrt{v_{xi}^2 + v_{yi}^2}. \tag{10}$$

Using $K_{\perp i}=K_{\perp 0}$ and $E_0=K_i$, it follows that

$$v_{z0} = \sqrt{v_{zi}^2 - \frac{2k_C q_1 q_2}{m_1 r_0}}. \tag{11}$$

The validity of $K_{\perp i}=K_{\perp 0}$ is verified in an approximate way by checking that $|K_{\perp c}-K_{\perp 0}|<0.01K_i$, where $K_{\perp c}=K_\perp(t=t_c)$, and the time period t_c is defined by $r(t_c)=\frac{1}{2}r_0$ with the condition that $r(t)$ decreases monotonically for $0<t<t_c$.

The following parameter values are used for a simulation named ATRAPsim: $B=5.4$ T, $T=4.2$ K, $x_g=1.5\times10^{-7}$ m, $\theta=0$, $\eta_x=1$, $\eta_y=1$, $\eta_z=1$, and $\zeta=100$. The values used for the magnetic field strength and the positron plasma temperature in ATRAPsim are consistent with the experimental parameters reported for the ATRAP experiment in Refs. [2,8]. Figure 2 shows the classical trajectory of an initially unbound positron that encounters an antiproton in the presence of a uniform magnetic field as computed by ATRAPsim. The direction of the magnetic field is indicated by the arrow, the

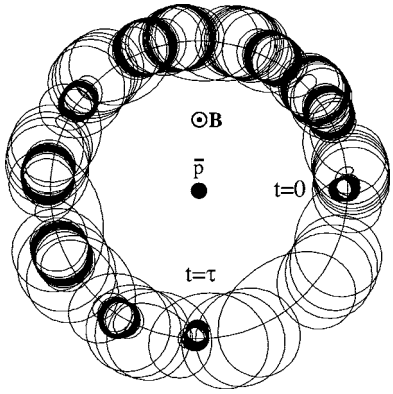

FIG. 3. The positron trajectory shown in Fig. 2, viewed from above. (Hence, $\boldsymbol{B}$ points out of the page.) A circle of radius x_g centered on the antiproton is also shown for comparison.

position of the antiproton is indicated by the large solid dot, the position of the positron when the simulation begins is labeled $t=0$, and the position of the positron when the simulation ends is labeled $t=\tau$. The positron is expected to leave the vicinity of the antiproton after time $t=\tau$. The plot of the positron trajectory is compressed in the dimension parallel to the magnetic field by a factor of 46 relative to the two dimensions perpendicular to the magnetic field. The interaction shown in Fig. 2 is an example of what is referred to here as a quasibound state. The positron crosses the $z=0$ plane 18 times. A positron will cross the $z=0$ plane no more than twice in simulations without a magnetic field. In consideration of this, a quasibound state is defined as a trajectory for which the positron crosses the $z=0$ plane three or more times.

For a sufficiently large distance of separation between the positron and antiproton, the positron experiences helical motion, and its guiding center does not move in the $\hat{\boldsymbol{i}}$ or $\hat{\boldsymbol{j}}$ directions noticeably. The pitch angle of the helical motion changes depending on the distance of separation between the two particles because the positron acquires kinetic energy as it gets lower in the potential energy well created by the antiproton's electric field. During times when the positron is near the $z=0$ plane, the positron guiding center drifts around the antiproton approximately along a circle of radius x_g. This $\boldsymbol{E}\times\boldsymbol{B}$ drift about the antiproton, which is shown in Fig. 3, occurs because the positron is pulled by the antiproton's electric field toward the antiproton across the magnetic field. For ATRAPsim, the size of the quasibound state in a dimension perpendicular to the magnetic field is approximately $2x_g=3\times10^{-7}$ m.

A positron constrained to move in one dimension will be trapped in a potential energy well only if its kinetic energy is less than the local well depth. (The term "local" refers to the positron's location.) Quasibound states may seem counterintuitive because the positron's kinetic energy is always greater than the local depth of the potential energy well. However, due to the presence of the magnetic field, the positron is confined (to cyclotron motion when sufficiently far from the antiproton) in the two dimensions perpendicular to the magnetic field. Confinement in the dimension parallel to the magnetic field can occur if the positron's parallel kinetic energy, which is defined as kinetic energy associated with motion parallel to the magnetic field, becomes less than the local well depth. Note that, of the well-defined helical paths that are observable in Fig. 2, the paths with the largest cyclotron radii are also those in which the positron travels the shortest distances away from the antiproton in the direction parallel to the magnetic field. A larger cyclotron radius indicates a larger perpendicular kinetic energy and a smaller parallel kinetic energy relative to the local well depth. The increase of the positron's perpendicular kinetic energy takes place in close vicinity to the antiproton. Such an increase causes a temporary reduction of the positron's parallel kinetic energy relative to the local well depth and results in turning points in the motion of the positron in the direction parallel to the magnetic field.

A simulation named ATHENAsim uses $B=3$ T, $T=15$ K, $x_g=1.9\times10^{-7}$ m, $\theta=0$, $\eta_x=1$, $\eta_y=1$, $\eta_z=1$, and $\zeta=100$, which also results in the formation of a quasibound state. The values of B and T used in ATHENAsim are consistent with the experimental parameters of the ATHENA experiment described in Refs. [1,3]. ATRAPsim and ATHENAsim are each continued up to a time τ, which is defined to be the first instant in time when the following three conditions are simultaneously met: $r(\tau)=r_0$, $r'(\tau)>0$, and $K_\perp(\tau)<K_i$. The first condition requires the distance of separation between the particles at $t=\tau$ to be the same as at $t=0$. The second condition requires the positron to be moving away from the antiproton at $t=\tau$. The third condition, which is written in terms of $K_\perp(\tau)$ for convenience, places a restriction on the minimum parallel kinetic energy at $t=\tau$. When the three conditions are simultaneously satisfied, the distance of separation is expected to increase monotonically for $t>\tau$, if the simulation were continued. The numerical differential equation solver in Mathematica is employed to numerically solve Eqs. (1)–(3). The total energy of the system, which should remain equal to K_i, changes as a result of numerical error by less than 0.11% in ATRAPsim and ATHENAsim. In contrast, the kinetic energy of the positron can increase substantially as it approaches the antiproton. For example, in ATRAPsim the positron kinetic energy reaches a value that is more than twenty times larger than K_i.

III. ANALYTICAL MODEL AND TIME SCALE COMPARISONS

Define b_{qbs} as the maximum value of x_g that produces a quasibound state. A corresponding maximum cross section for the formation of quasibound states is $\sigma_{qbs}=\pi b_{qbs}^2$, which applies for $r_c \ll b_{qbs}$ and which can be used as an approximate cross section. An analytical expression for b_{qbs} is now derived by considering a simple model based on a comparison of time scales and based on the approximation, $r_c \ll x_g$. A quasibound state forms when an increase of the positron's perpendicular kinetic energy takes place in close vicinity to the antiproton. Similar increases have been discussed in detail for collisional interactions within pure electron plasmas [22,23]. In consideration of the finding reported in Refs. [22,23], an increase of the positron's perpendicular kinetic

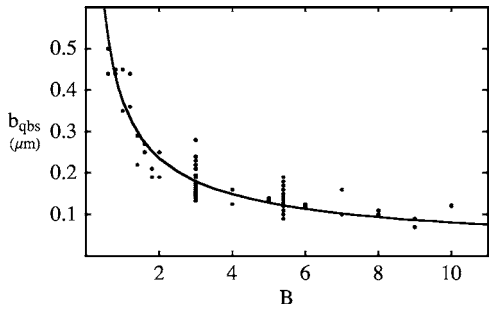

FIG. 4. A comparison of b_{qbs} values according to simulation results and Eq. (12) using $C=1.86$.

energy is considered to occur only when the time scale, $\Delta t = x_g / v|_{z=0}$, is smaller than the cyclotron period, $\tau_c = 2\pi m_1/(k_L q_1 B)$. The time scale associated with the changing local well depth must be small enough for the cyclotron adiabatic invariant to be broken. The speed of the positron at $z=0$ is approximated as $v|_{z=0}=[2k_C q_1|q_2|/(m_1 x_g)]^{1/2}$, which amounts to assuming that the kinetic energy of the positron at $z=0$ is much larger than K_i. Taking $\Delta t < \tau_c$ to be the criterion for a quasibound state to form, it follows that

$$b_{qbs1} = C\left(\frac{k_C m_1}{k_L^2 B^2}\right)^{1/3} \tag{12}$$

represents an upper limit on x_g for which a quasibound state can form. Here $q_1=|q_2|$ has been used, and C has been incorporated as a constant that has a value of order unity. It is interesting to note that a scale length that is the same as Eq. (12) with $C=1$ has been used to establish a criterion associated with guiding center drift atoms, which are weakly bound atoms with electron dynamics that can be described using guiding center drift theory [14].

The dependence of b_{qbs} on η_x, η_y, η_z, θ, B, and T is explored in two sets of simulations. Except for variations done on a single parameter value, one set of simulations uses the ATRAPsim parameters and the other set uses the ATHENAsim parameters. The variations done on a single parameter value are as follows: The value of $\eta_x=\eta_y$ is varied from 0 to 2 in increments of 0.2. The value of η_z is varied between 0 and 3 in increments of 0.2. The value of θ is varied between 0 and 1.8π in increments of 0.2π. The value of B is varied from 0.6 to 2 T in increments of 0.2 T and from 3 to 10 T in increments of 1 T. The value of T is varied from 1 to 10 K in increments of 1 K and from 20 to 60 K in increments of 10 K. It should be noted that the parameter study reported here represents an extension of the range and accuracy of the previously reported parameter study [21]. Figure 4 shows a comparison of the results of the parameter study and Eq. (12) using $C=1.86$. Equation (12) is found to agree with the simulation results to within an accuracy of 37%.

The dependence of τ on x_g is explored in two other sets of simulations. The positron trajectory is repeatedly computed using ATRAPsim and ATHENAsim parameters, respectively, except with x_g varied from 5×10^{-8} m to 2.1×10^{-7} m in increments of 1×10^{-8} m and with θ values of 0, $\pi/2$, π, and $3\pi/2$. The ratio $\tau/\tau_{B=0}$ is plotted in Fig. 5, where $\tau_{B=0}$ refers to the value of τ in the absence of a magnetic field and using $\eta_x=\eta_y=0$ and $r_c=0$. The results indicate that the formation of quasibound states can increase the positron and antiproton interaction time substantially compared to the interaction time in the absence of an external magnetic field. The ratio $\tau/\tau_{B=0}$ is approximately 1 for x_g larger than about 2×10^{-7} m. The size of a quasibound antihydrogen state in a dimension perpendicular to the magnetic field is typically less than 4×10^{-7} m for ATRAP and ATHENA experimental parameters.

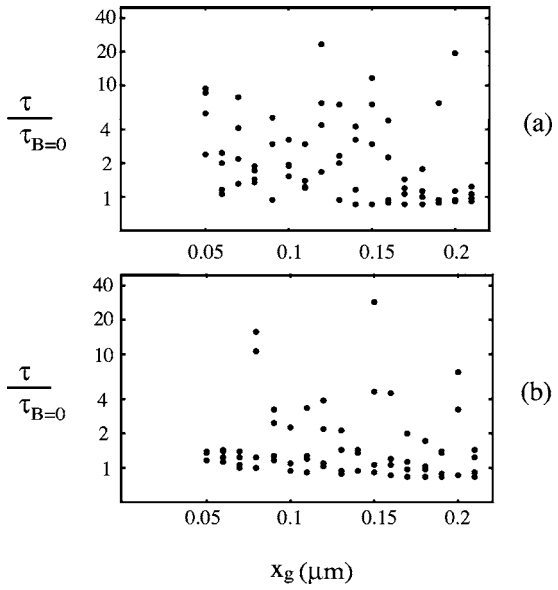

FIG. 5. Semilogarithmic plot of $\tau/\tau_{B=0}$ according to ATRAPsim (a) and ATHENAsim (b) with x_g varied from 5×10^{-8} to 2.1×10^{-7} m and with θ values of 0, $\pi/2$, π, and $3\pi/2$. Three values of $\tau/\tau_{B=0}$ (not shown) are over 50.

The expression,

$$b_{qbs2} = \sqrt{\frac{k_C|q_2|}{k_L v_i B}}, \tag{13}$$

which was previously arrived at by using what may be considered a phenomenological approach, was found to agree with simulation results to within an accuracy of 39% [21]. Equation (13) provides a convenient expression for estimating the rate of formation of quasibound antihydrogen states. Using Eq. (13) for b_{qbs}, an approximate time scale for the formation of quasibound states is found to be

$$\tau_{qbs} = \frac{1}{n\langle\sigma_{qbs} v_i\rangle} = \frac{k_L B}{\pi k_C |q_2| n}, \tag{14}$$

where n is the positron density, the average is over the velocity distribution of the positrons, and antiproton motion is neglected. Note that τ_{qbs} is independent of the plasma temperature because v_i within the velocity average cancels out. Not all interactions with $x_g < b_{qbs}$ form quasibound states. For example, 16 trajectories out of 80 were *not* qua-

sibound states for the results in Fig. 5 for $x_g \leqslant 1.4\times10^{-7}$ m. ($b_{qbs2}=1.4\times10^{-7}$ m for both ATRAPsim and ATHENAsim parameters used in Fig. 5.) Hence, the actual time scale for quasibound state formation may be somewhat larger than τ_{qbs}. Nevertheless, it is worthwhile to compare Eq. (14) to the time scales for other processes. For example, the time scale associated with three-body recombination that produces Rydberg atoms with sufficient binding energy to be stable (to avoid reionization) in the positron plasma has been found to approximately be [16]

$$\tau_{tbr}=\frac{1.8\times10^{21}T^{9/2}}{n^2} \tag{15}$$

for typical ATRAP and ATHENA experimental parameter values. Using Eqs. (14) and (15), and with the simulation results, the following relationship is found for typical ATRAP and ATHENA experimental parameter values: $\tau \ll \tau_{qbs} \ll \tau_{tbr}$. For typical ATRAP experimental parameters $(B,T,n)=(5.4\text{ T}, 4.2\text{ K}, 1.5\times10^{13}\text{ m}^{-3})$, time scale values are $(\tau,\tau_{qbs},\tau_{tbr})=(7.3\times10^{-9}\text{ s}, 8.0\times10^{-5}\text{ s}, 5.1\times10^{-3}\text{ s})$, where the value of τ is from ATRAPsim, and the positron density is from Ref. [24]. For typical ATHENA experimental parameters $(B,T,n)=(3\text{ T}, 15\text{ K}, 1.7\times10^{14}\text{ m}^{-3})$, time scale values are $(\tau,\tau_{qbs},\tau_{tbr})=(2.7\times10^{-9}\text{ s}, 3.9\times10^{-6}\text{ s}, 1.2\times10^{-2}\text{ s})$, where the value of τ is from ATHENAsim, and the positron density is from Ref. [3].

IV. DISCUSSION AND CONCLUDING SUMMARY

The relationship $\tau_{qbs} \ll \tau_{tbr}$ indicates that quasibound states may form more frequently than stable Rydberg states in antihydrogen production experiments. In fact, the formation of quasibound states may affect antihydrogen production experiments by affecting the three-body recombination rate. The three-body recombination process begins when an initially unbound positron passes near an antiproton, while a second positron is also near, and enough energy is transferred to the second positron for the first positron and the antiproton to form an atom. The formation of a quasibound state may increase the time a positron resides near an antiproton and the probability for a second positron to be near enough to take part in the three-body recombination process. It should be possible, in principle, to predict whether the formation of quasibound states affects the three-body recombination rate by simulating two positrons and an antiproton interacting with each other and conducting a Monte Carlo study similar to that in Ref. [16]. However, it may be difficult to manage the computation time if the full three-dimensional positron motion is computed. It would also be instructive to have experimental measurements of the dependence of three-body recombination on magnetic field strength under conditions where the analytical model presented here applies (i.e., for $r_c \ll b_{qbs}$). The results of such measurements may provide indications of whether quasibound state formation has a noticeable effect on three-body recombination. It should be noted that, in analyzing the results of such measurements, the possible effect of arrested three-body capture [17], which occurs if newly formed atoms do not remain within the plasma for sufficient time, must be considered.

The formation of quasibound states may affect the rate of diffusion of positrons across a magnetic field. Positron diffusion transverse to a magnetic field occurs, in part, because the guiding center position of a positron shifts with each binary interaction between a positron and an antiproton. The shift associated with a single binary interaction is normally not larger than a typical cyclotron radius. Figure 2 shows that the cyclotron radius at $t=0$ is much smaller than the distance of separation between the guiding center position at $t=0$ and the guiding center position at $t=\tau$. The simulation indicates that a binary interaction that results in the formation of a quasibound state can cause a shift of the positron guiding center that is much larger than the cyclotron radius before the interaction.

An understanding of the effect that the formation of quasibound states may have on three-body recombination and positron diffusion remains to be developed. An understanding of the effect that antiproton motion may have on the formation and duration of quasibound states also remains to be developed. It might be expected that for antiproton motion parallel to the magnetic field, if the antiproton speed is much less than the positron thermal speed, the results presented here regarding the formation and duration of quasibound states would continue to apply. In fact, it is interesting to note that Eq. (12) shows no dependence on v_{zi}. It might also be expected that for antiproton motion perpendicular to the magnetic field, if the antiproton speed is much less than the positron thermal speed, the results presented here regarding the formation, but not necessarily the duration, of quasibound states would continue to apply. To derive Eq. (12), an increase of the positron's perpendicular kinetic energy was considered to occur during a time period smaller than the positron cyclotron period. If the antiproton speed perpendicular to the magnetic field is much less than the positron thermal speed, then the antiproton will move a distance much less than the positron cyclotron radius during a time period smaller than the positron cyclotron period. It should also be mentioned that, because a future goal of antihydrogen production experiments is to trap antihydrogen in a magnetic well, antiproton temperatures less than ≈ 1 K will be needed, and nested Penning traps may be operated with the antiprotons having a temperature that is much smaller than that of the positrons [5].

In summary, classical trajectory simulations indicate the formation of quasibound states of antihydrogen under conditions reported in recent antihydrogen production experiments. An expression that can be used to predict an approximate cross section for the formation of quasibound antihydrogen states was derived, and reasonable agreement with simulation results was found for the parameters considered. The time a positron and antiproton interact while in a quasibound state was found in many cases to be much greater than the interaction time in the absence of an external magnetic field. An expression for an approximate time scale associated with the rate of formation of quasibound antihydrogen states was obtained. It was found that quasibound states may form more frequently than stable Rydberg states in antihydrogen production experiments.

ACKNOWLEDGMENTS

The authors would like to thank S. A. Khan and Dr. Y. Chang for early contributions to the work and Profs. A. Dalgarno and D. Weathers for helpful comments. This material is based upon work supported by the National Science Foundation under an REU program and under Grant No. PHY-0244444.

[1] M. Amoretti, C. Amsler, G. Bonomi, A. Bouchta, P. Bowe, C. Carraro, C. L. Cesar, M. Charlton, M. J. T. Collier, M. Doser, V. Filippini, K. S. Fine, A. Fontana, M. C. Fujiwara, R. Funakoshi, P. Genova, J. S. Hangst, R. S. Hayano, M. H. Holzscheiter, L. V. Jorgensen, V. Lagomarsino, R. Landua, D. Lindelof, E. Lodi Rizzini, M. Macri, N. Madsen, G. Manuzio, M. Marchesotti, P. Montagna, H. Pruys, C. Regenfus, P. Riedler, J. Rochet, A. Rotondi, G. Rouleau, G. Testera, A. Variola, T. L. Watson, and D. P. van der Werf, Nature (London) **419**, 456 (2002).

[2] G. Gabrielse, N. S. Bowden, P. Oxley, A. Speck, C. H. Storry, J. N. Tan, M. Wessels, D. Grzonka, W. Oelert, G. Schepers, T. Sefzick, J. Walz, H. Pittner, T. W. Hansch, and E. A. Hessels, Phys. Rev. Lett. **89**, 213401 (2002).

[3] M. Amoretti, C. Amsler, G. Bazzano, G. Bonomi, A. Bouchta, P. D. Bowe, C. Canali, C. Carraro, C. L. Cesar, M. Charlton, M. Doser, A. Fontana, M. C. Fujiwara, R. Funakoshi, P. Genova, J. S. Hangst, R. S. Hayano, I. Johnson, L. V. Jorgensen, A. Kellerbauer, V. Lagomarsino, R. Landua, E. Lodi Rizzini, M. Macri, N. Madsen, G. Manuzio, M. Marchesotti, D. Mitchard, F. Ottone, H. Pruys, C. Regenfus, P. Riedler, A. Rotondi, G. Testera, A. Variola, L. Venturelli, Y. Yamazaki, D. P. van der Werf, and N. Zurlo, Phys. Lett. B **583**, 59 (2004).

[4] J. N. Tan, N. S. Bowden, G. Gabrielse, P. Oxley, A. Speck, C. H. Storry, M. Wessels, D. Grzonka, W. Oelert, G. Schepers, T. Sefzick, J. Walz, H. Pittner, T. W. Hansch, and E. A. Hessels, Nucl. Instrum. Methods Phys. Res. B **214**, 22 (2004).

[5] C. A. Ordonez, D. D. Dolliver, Y. Chang, and J. R. Correa, Phys. Plasmas **9**, 3289 (2002).

[6] D. D. Dolliver and C. A. Ordonez, Phys. Rev. E **62**, 5855 (2000).

[7] D. D. Dolliver and C. A. Ordonez, Phys. Rev. E **59**, 7121 (1999).

[8] G. Gabrielse, N. S. Bowden, P. Oxley, A. Speck, C. H. Storry, J. N. Tan, M. Wessels, D. Grzonka, W. Oelert, G. Schepers, T. Sefzick, J. Walz, H. Pittner, T. W. Hänsch, and E. A. Hessels, Phys. Rev. Lett. **89**, 233401 (2002).

[9] M. E. Glinsky and T. M. O'Neil, Phys. Fluids B **3**, 1279 (1991).

[10] E. M. Bass and D. H. E. Dubin, Phys. Plasmas **11**, 1240 (2004).

[11] L. I. Menshikov and P. O. Fedichev, JETP **81**, 78 (1995).

[12] P. O. Fedichev, Phys. Lett. A **226**, 289 (1997).

[13] S. G. Kuzmin and T. M. O'Neil, Phys. Rev. Lett. **92**, 243401 (2004).

[14] S. G. Kuzmin, T. M. O'Neil, and M. E. Glinsky, Phys. Plasmas **11**, 2382 (2004).

[15] D. Vrinceanu, B. E. Granger, R. Parrott, H. R. Sadeghpour, L. Cederbaum, A. Mody, J. Tan, and G. Gabrielse, Phys. Rev. Lett. **92**, 133402 (2004).

[16] F. Robicheaux and J. D. Hanson, Phys. Rev. A **69**, 010701(R) (2004).

[17] F. Robicheaux, Phys. Rev. A **70**, 022510 (2004).

[18] S. G. Kuzmin and T. M. O'Neil, Phys. Plasmas **12**, 012101 (2005).

[19] B. Hu, W. Horton, C. Chiu, and T. Petrosky, Phys. Plasmas **9**, 1116 (2002).

[20] B. Hu, W. Horton, and T. Petrosky, Phys. Rev. E **65**, 056212 (2002).

[21] C. E. Correa, S. A. Khan, J. R. Correa, and C. A. Ordonez, Nucl. Instrum. Methods Phys. Res. B (to be published).

[22] T. M. O'Neil and P. G. Hjorth, Phys. Fluids **28**, 3241 (1985).

[23] M. E. Glinsky, T. M. O'Neil, M. N. Rosenbluth, K. Tsuruta, and S. Ichimaru, Phys. Fluids B **4**, 1156 (1992).

[24] G. Gabrielse, N. S. Bowden, P. Oxley, A. Speck, C. H. Storry, J. N. Tan, M. Wessels, D. Grzonka, W. Oelert, G. Schepers, T. Sefzick, J. Walz, H. Pittner, T. W. Hänsch, and E. A. Hessels, Phys. Rev. Lett. **92**, 149304 (2004).